

## Evolution of Beam Distribution in Crossing a Walkinshaw Resonance

S. Y. Lee,<sup>1</sup> K. Y. Ng,<sup>2</sup> H. Liu,<sup>1</sup> and H. C. Chao<sup>1</sup>

<sup>1</sup>*Department of Physics, Indiana University, Bloomington, Indiana 47405, USA*

<sup>2</sup>*Fermilab, P. O. Box 500, Batavia, Illinois 60510, USA*

(Received 10 November 2012; published 28 February 2013)

The third-integer coupling resonance at  $\nu_x - 2\nu_z = \ell$ , known as the Walkinshaw resonance, is important in high-power accelerators. We find that, when the betatron tunes ramp through a Walkinshaw resonance the fractional emittance growth (FEG) is a universal function of the effective resonance strength:  $G_{1,-2,\ell} \sqrt{\epsilon_{xi}} |\Delta(\nu_x - 2\nu_z)/\Delta n|^{-1/2}$ , where  $G_{1,-2,\ell}$  is the resonance strength;  $\epsilon_{xi}$  and  $\epsilon_{zi}$  are the initial horizontal and vertical emittances, respectively; and  $|\Delta(\nu_x - 2\nu_z)/\Delta n|$  is the resonance crossing rate per revolution. At large effective resonance strengths, the FEG reaches an asymptotic maximum value  $(\text{FEG})_{\text{max}} \sim 2\epsilon_{xi}/\epsilon_{zi}$  for  $\epsilon_{xi} \gg \frac{1}{2}\epsilon_{zi}$  or  $\epsilon_{zi}/(2\epsilon_{xi})$  for  $\epsilon_{xi} \ll \frac{1}{2}\epsilon_{zi}$ . There is little emittance exchange at  $\epsilon_{xi} = \frac{1}{2}\epsilon_{zi}$ , which can be used to minimize emittance growth in crossing a Walkinshaw resonance.

DOI: 10.1103/PhysRevLett.110.094801

PACS numbers: 29.20.-c, 41.60.Ap, 41.85.-p

Low-order coupling resonances are of concern to the design and operation of circular accelerators. The third-integer difference resonance  $\nu_x - 2\nu_z = \ell$ , known as the Walkinshaw resonance, is sometimes unavoidable in many high-power accelerators, such as isochronous cyclotrons, nonscaling fixed field alternating gradients, and other low-energy accelerators. This resonance becomes a focus of the design and operation of all cyclotrons [1]. It has been termed a “formidable barrier” and “impassable” [2] and may cause emittance growths and beam loss. Although all the adverse effects of the resonance have long been experienced, the dynamic of emittance growths, however, has not been fully analyzed and understood. So far, the only means of reducing emittance growths have been fast passage and the reduction of the resonance strength.

There had been theoretical analysis on the  $\nu_x - 2\nu_z = \ell$  resonance [2,3] and subsequent experimental measurements in storage rings [4,5]. These papers, however, deal essentially with single-particle motion near the resonance at fixed betatron tunes. This Letter investigates instead the beam dynamics while the betatron tunes ramp through the third-integer coupling resonance. We study emittance growths and scaling laws. Methods are given to alleviate the emittance growth.

In term of the horizontal and vertical action-angle phase-space coordinates  $(J_x, \phi_x)$  and  $(J_z, \phi_z)$ , the Hamiltonian near the  $\nu_x - 2\nu_z = \ell$  resonance can be approximated as [5,6]

$$H = \nu_x J_x + \nu_z J_z + \frac{1}{2} \alpha_{xx} J_x^2 + \alpha_{xz} J_x J_z + \frac{1}{2} \alpha_{zz} J_z^2 + G_{1,-2,\ell} J_x^{1/2} J_z \cos(\phi_x - 2\phi_z - \ell\theta + \xi_{1,-2,\ell}) + \dots$$

Here, the orbiting angle  $\theta = s/R$  serves as the “time coordinate”;  $R$  is the mean radius;  $\nu_x$  and  $\nu_z$  are, respectively, the horizontal and vertical betatron tunes;  $\ell$  is an integer; and the nonlinear detuning parameters are

$$\alpha_{xx,zz} = - \oint \frac{\beta_{x,z}^2 B_z'''(s)}{16\pi B\rho} ds, \quad \alpha_{xz} = \oint \frac{\beta_x \beta_z B_z'''(s)}{8\pi B\rho} ds.$$

The resonance strength  $G_{1,-2,\ell} \geq 0$  and its phase  $\xi_{1,-2,\ell}$  are represented by

$$G_{1,-2,\ell} e^{j\xi_{1,-2,\ell}} = \frac{\sqrt{2}}{8\pi} \oint \beta_x^{1/2} \beta_z \frac{B_z''(s)}{B\rho} \times e^{j[\chi_x(s) - 2\chi_z(s) - (\nu_x - 2\nu_z - \ell)\theta]} ds,$$

where  $\beta_{x,y}$  and  $\chi_{x,y}(s) = \int_0^s ds' / \beta_{x,y}(s')$  are the horizontal or vertical betatron functions and betatron phases. In the above equation,  $B_z''$  and  $B_z'''$  are, respectively, the sextupole and octupole magnetic field components around the ring, with  $B\rho$  representing the rigidity of the beam.

The Hamiltonian is canonically transformed to the rotating frame using the generating function

$$F_2(\phi_x, \phi_z, J_1, J_2) = (\phi_x - 2\phi_z - \ell\theta + \xi_{1,-2,\ell})J_1 + \phi_z J_2.$$

The coordinate transformation is

$$\begin{aligned} \phi_1 &= \phi_x - 2\phi_z - \ell\theta + \xi_{1,-2,\ell}, & J_x &= J_1, \\ \phi_2 &= \phi_z, & J_z &= -2J_1 + J_2, \end{aligned}$$

and the new Hamiltonian becomes  $\tilde{H} = H_1(J_1, \phi_1, J_2) + H_2(J_2)$ , where  $H_2(J_2) = \nu_z J_2 + \frac{1}{2} \alpha_{22} J_2^2$  and

$$H_1(J_1, \phi_1, J_2) = \delta J_1 + \frac{1}{2} \alpha_{11} J_1^2 + \alpha_{12} J_1 J_2 + G_{1,-2,\ell} J_1^{1/2} (J_2 - 2J_1) \cos(\phi_1). \quad (1)$$

Here,  $\delta = \nu_x - 2\nu_z - \ell$  is the resonance proximity parameter, and the transformed detuning parameters are  $\alpha_{11} = \alpha_{xx} - 4\alpha_{xz} + 4\alpha_{zz}$ ,  $\alpha_{12} = \alpha_{xz} - 2\alpha_{zz}$ , and  $\alpha_{22} = 4\alpha_{zz}$ . Hamilton's equations of motion are  $\frac{dJ_2}{d\theta} = -\frac{\partial \tilde{H}}{\partial \phi_2} = 0$ ,  $\frac{d\phi_2}{d\theta} = \frac{\partial \tilde{H}}{\partial J_2}$ , and

$$\frac{dJ_1}{d\theta} = -\frac{\partial \tilde{H}}{\partial \phi_1} = G_{1,-2,\ell} J_1^{1/2} (J_2 - 2J_1) \sin(\phi_1), \quad (2)$$

$$\begin{aligned} \frac{d\phi_1}{d\theta} = & +\frac{\partial \tilde{H}}{\partial J_1} = \delta + \alpha_{12} J_2 + \alpha_{11} J_1 \\ & + G_{1,-2,\ell} \frac{J_2 - 6J_1}{2J_1^{1/2}} \cos(\phi_1). \end{aligned} \quad (3)$$

Particle dynamics obey Eqs. (2) and (3) at constant  $J_2$  and  $H_1$ , which are invariants if the betatron tunes are not changed. However, we study the dynamics of particle motion during the passage of a resonance. Even when the betatron tunes are ramped,  $J_2$  remains an invariant. In reality, particle motion is under the influence of many other resonances;  $J_2$  is quasi-invariant. Since the rate of resonance crossing is normally small,  $H_1$  changes slowly. Particle motion follows a quasiconstant  $H_1$  contour.

The fixed points of the Hamiltonian  $H_1$  are obtained by equating both Eqs. (2) and (3) to zero. Two unstable fixed points (UFPs) are located at the intersections between the Courant-Snyder (CS) circle ( $2J_1 = J_2$ ) and the coupling arc. Separatrices at other various conditions have been shown in Ref. [3]. Figure 2 in Ref. [5] also shows the experimental data of one of the separatrices for this resonance, where the CS and coupling circles are expressed in phase-space coordinates  $(X, P) = (\sqrt{2\beta_x J_1} \cos \phi_1, -\sqrt{2\beta_x J_1} \sin \phi_1)$ , with  $\beta_x$  being the horizontal betatron function at the observation point. The separatrix is the Hamiltonian torus that passes through the unstable fixed points; i.e.,

$$\begin{aligned} \frac{1}{2}(J_2 - 2J_1) \left\{ -\delta - \frac{1}{2}\alpha_{11} \left( J_1 + \frac{J_2}{2} \right) \right. \\ \left. - \alpha_{12} J_2 + 2G_{1,-2,\ell} J_1^{1/2} \cos(\phi_1) \right\} = 0, \end{aligned}$$

which is composed of a CS circle  $2J_1 = J_2$  and a coupling arc  $\alpha_{11}(2J_1) - 4\sqrt{2}G_{1,-2,\ell}\sqrt{2J_1}\cos\phi_1 + 4\delta + 4\alpha_{12}J_2 + \alpha_{11}J_2 = 0$ . For particles with  $2J_1 < J_2$ , their flows revolve around the stable fixed points at  $\phi = 0$  or  $\pi$ , and  $2\alpha_{11}J_1^{3/2} \mp 6G_{1,-2,\ell}J_1 + 2(\delta + \alpha_{12}J_2)J_1^{1/2} \pm G_{1,-2,\ell}J_2 = 0$ . Experimental data depicting the Hamiltonian flow of these particles have been shown in Fig. 7 of Ref. [5].

Now, we study the effects of the Walkinshaw resonance on a beam of particles. When the betatron tunes ramp through a Walkinshaw resonance, all fixed points move across the beam, and the beam distribution will evolve as well. Consider a beam with bi-Gaussian distribution

$$\rho_2(J_x, J_z) = \frac{1}{\epsilon_x \epsilon_z} \exp\left\{-\frac{J_x}{\epsilon_x} - \frac{J_z}{\epsilon_z}\right\}, \quad (4)$$

where  $\epsilon_x$  and  $\epsilon_z$  are, respectively, the horizontal and vertical rms emittances of the beam [6]. Now,  $J_x$  and  $J_z$  are transformed to  $J_1$  and  $J_2$ . The invariant distribution function in  $J_2$  can be obtained by integrating over  $J_1$ :

$$\rho_1(J_2) = \frac{1}{2\epsilon_x - \epsilon_z} \left[ \exp\left(-\frac{J_2}{2\epsilon_x}\right) - \exp\left(-\frac{J_2}{\epsilon_z}\right) \right]. \quad (5)$$

As the betatron tunes ramp through the  $\nu_x - 2\nu_z = \ell$  resonance, the action  $J_2$  is invariant, and the distribution function  $\rho_1(J_2)$  is invariant. The first moment  $\langle J_2 \rangle = 2\epsilon_x + \epsilon_z$  is also invariant, and thus  $\Delta\epsilon_z = -2\Delta\epsilon_x$ . For the above bi-Gaussian distribution, the maximum of the invariant distribution function occurs at

$$J_{2,\max} = \frac{2\epsilon_x \epsilon_z}{2\epsilon_x - \epsilon_z} \ln \frac{2\epsilon_x}{\epsilon_z}.$$

Since  $J_2$  varies from particle to particle, it is advantageous to study the beam distribution in the variable  $u = J_1/J_2$ . The transformed beam distribution is

$$\rho_{2a}(u, J_2) = \frac{J_2}{\epsilon_x \epsilon_z} \exp\left\{-\left(\frac{u}{\epsilon_x} + \frac{1-2u}{\epsilon_z}\right)J_2\right\}, \quad (6)$$

where the variables  $u \in [0, \frac{1}{2}]$  and  $J_2 \in [0, \infty]$ . In this representation, all particles in the beam have the same CS circle at  $u = J_1/J_2 = 1/2$ . We also note that, when  $\epsilon_x = \frac{1}{2}\epsilon_z$ ,  $\rho_{2a}(u, J_2)$  is independent of  $u$  for all  $J_2$ . Integrating over  $J_2$ , we find the 1D distribution as

$$\rho_{1a}(u) = \frac{\epsilon_x/\epsilon_z}{[\epsilon_x/\epsilon_z + (1-2\epsilon_x/\epsilon_z)u]^2} \Theta\left(\frac{1}{2} - u\right), \quad (7)$$

where  $\Theta$  is the Heaviside step function. Figure 1 shows Eq. (7) for the bi-Gaussian distribution. When  $\epsilon_{xi} > \frac{1}{2}\epsilon_{zi}$ , there are more particles at higher  $J_1$  actions, and we expect that the horizontal emittance will decrease in crossing a Walkinshaw resonance. Conversely, when  $\epsilon_{xi} < \frac{1}{2}\epsilon_{zi}$ , the horizontal emittance will increase in crossing the Walkinshaw resonance. At the condition  $\epsilon_{xi} = \frac{1}{2}\epsilon_{zi}$ , the distribution function is uniform, and we expect no emittance exchange during the crossing of a Walkinshaw resonance.

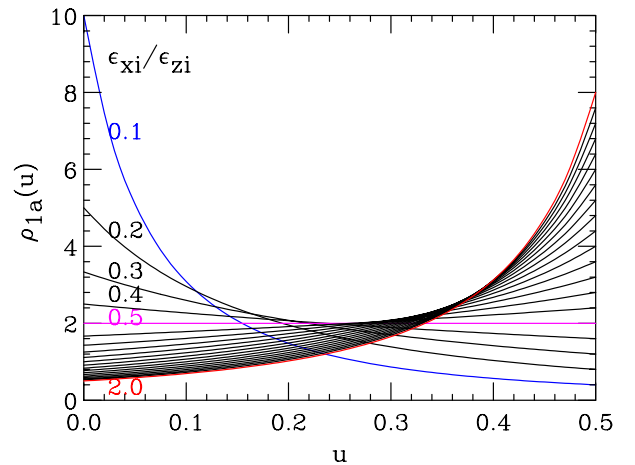


FIG. 1 (color online). The distribution of a bi-Gaussian beam in the  $u = J_1/J_2$  action coordinate for various horizontal and vertical emittance ratios  $\epsilon_{xi}/\epsilon_{zi} = 0.1, 0.2, \dots, 2.0$ . If  $\epsilon_{xi} > \frac{1}{2}\epsilon_{zi}$ , there are more particles with higher  $J_1 = J_x$  actions, and vice versa. The distribution is uniform when  $\epsilon_{xi} = \frac{1}{2}\epsilon_{zi}$ .

When the betatron tunes ramp through a  $\nu_x - 2\nu_z = \ell$  resonance with  $\epsilon_{xi} > \frac{1}{2}\epsilon_{zi}$ , there are more particles with higher horizontal actions. They are drawn along the coupling arc toward the center of the CS circle with their horizontal actions reduced and vertical actions increased. With  $2\Delta\epsilon_x + \Delta\epsilon_z = 0$ , the *fractional emittance growth* (FEG), defined below, has the properties [7]

$$\begin{aligned} \text{FEG} &\equiv \left| \frac{\Delta\epsilon_x}{\epsilon_{xi}} \right| + \left| \frac{\Delta\epsilon_z}{\epsilon_{zi}} \right| = \left| \frac{\Delta\epsilon_x}{\epsilon_{xi}} \right| \left( \frac{2\epsilon_{xi}}{\epsilon_{zi}} + 1 \right) \\ &= \left| \frac{\Delta\epsilon_z}{\epsilon_{zi}} \right| \left( \frac{\epsilon_{zi}}{2\epsilon_{xi}} + 1 \right). \end{aligned} \quad (8)$$

Multiparticle simulations were performed to study the dynamics of resonance crossing. Details of these simulations have been published in Ref. [8]. Macroparticles, typically 5000, are populated in a bi-Gaussian distribution with initial rms emittances  $\epsilon_{xi}$  and  $\epsilon_{zi}$ . The rms beam emittances are computed by using the second moments of the phase-space distributions [6] at each revolution. Sextupoles are used to control the strength of the Walkinshaw resonance, and octupoles are used to control the detuning parameters. The betatron tunes are varied linearly to cross a  $\nu_x - 2\nu_z = \ell$  resonance. Figure 2 shows the evolution of the horizontal and vertical emittances during the crossing the resonance, with  $\alpha_{11}$  ranging from  $-2000$  to  $+2000$   $(\pi\text{m})^{-1}$ , which corresponds to a tune spread of  $6\alpha_{11}\epsilon_{xi} \approx 0.060$  within the beam.

The beam may encounter the resonance earlier or later, depending on the detuning parameters, but the final FEGs are nearly independent of the detuning parameters. Simulations with larger emittances will reach the same conclusion. In fixed field alternating gradient accelerators and cyclotrons, the ramp rates depend on the available rf voltage and quadrupole ramping rate. One would try to

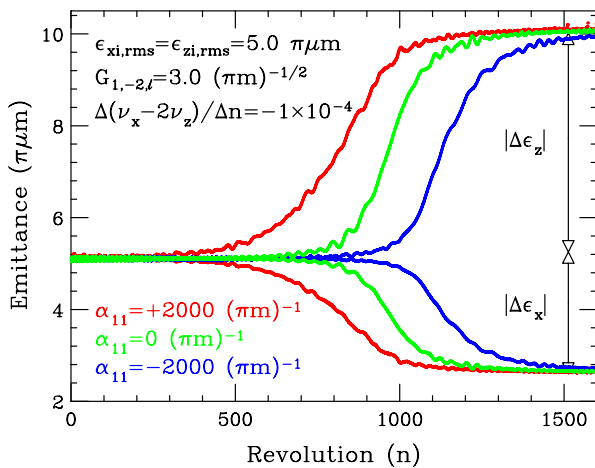


FIG. 2 (color online). The resonance crossing rate is  $-1.0 \times 10^{-4}$  for a third-integer difference resonance with resonance strength  $G_{1,-2,\ell} = 3.0$   $(\pi\text{m})^{-1/2}$  and  $\epsilon_{xi} = \epsilon_{zi} = 5.0$   $\pi\mu\text{m}$ . The detuning parameters are  $\alpha_{11} = 0$  and  $\pm 2000$   $(\pi\text{m})^{-1}$ .

ramp through the resonances as fast as possible to avoid adverse effects. The typical tune-ramp rate is about  $10^{-5}$ – $10^{-3}$  per revolution, and we use these typical tune-ramp rates in our simulations. At these tune-ramp rates, particle motion follows the Hamiltonian flow or the motion is “adiabatic.”

Now, we study the scaling properties of the FEG vs accelerator parameters. Figure 3 shows results of simulations with  $\epsilon_{xi} = \epsilon_{zi}$ . The FEGs depend essentially on a single effective resonance strength parameter  $G_{\text{eff}} = G_{1,-2,\ell}\sqrt{\epsilon_{xi}}/\sqrt{|\Delta(\nu_x - 2\nu_z)/\Delta n|}$  but are independent of detuning parameters. Note that the maximum FEG for equal initial emittances is about 1.5. This means that the maximum fractional emittance growth in the vertical plane is about 1.0 and that the maximum fractional horizontal emittance reduction is about 0.5.

Figure 1 shows that there are more particles in lower  $J_1$  actions when  $\epsilon_{xi} < \frac{1}{2}\epsilon_{zi}$ . Thus, the horizontal emittance will increase and the vertical emittance will decrease. Figure 4 shows the emittance exchange for  $\epsilon_{xi} = 1$   $\pi\mu\text{m}$ , and  $\epsilon_{zi} = 10$   $\pi\mu\text{m}$  with  $|\Delta(\nu_x - 2\nu_z)/\Delta n| = 8 \times 10^{-5}$ . The horizontal emittance increases while the vertical emittance decreases with the FEG  $\sim 4.5$ .

According to the FEG scaling law in Eq. (8), when  $2\epsilon_{xi} \gg \epsilon_{zi}$ , the maximum FEG is  $\sim 2\epsilon_{xi}/\epsilon_{zi}$ , and, when  $2\epsilon_{xi} \ll \epsilon_{zi}$ , the maximum FEG is  $\sim \epsilon_{zi}/(2\epsilon_{xi})$ . Figure 5 gathers a large amount of simulation data, depicting the maximum FEG vs  $\epsilon_{xi}/\epsilon_{zi}$ . The dashed and dotted lines show the asymptotic maxima FEG =  $2\epsilon_{xi}/\epsilon_{zi}$  and  $\epsilon_{zi}/(2\epsilon_{xi})$  of Eq. (8). At  $\epsilon_{xi} \approx \frac{1}{2}\epsilon_{zi}$ , there is little emittance exchange. Although Fig. 1 is based on bi-Gaussian distribution, the FEG scaling law works for other distributions as well. The circle, rectangular, and diamond symbols in Fig. 5 represent results for a beam with an initial uniform beam distribution in both or one of the

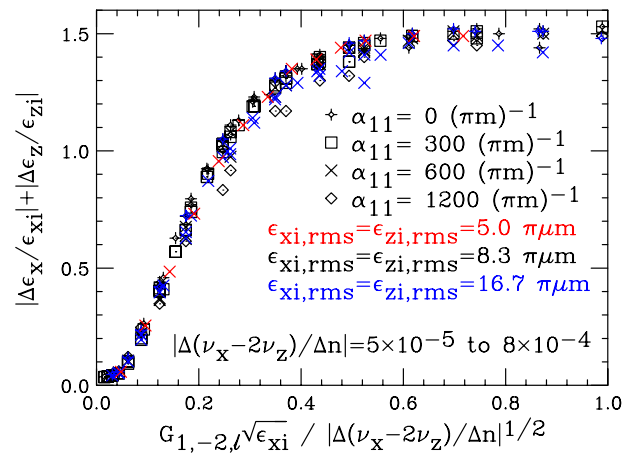


FIG. 3 (color online). The FEG vs the effective resonance parameter for initially equal-emittance Gaussian-distributed beams. Note that the FEG depends only on a single effective resonance strength:  $G_{1,-2,\ell}\sqrt{\epsilon_{xi}}/\sqrt{|\Delta(\nu_x - 2\nu_z)/\Delta n|}$ . The FEGs are independent of the detuning parameters  $\alpha_{11}$ .

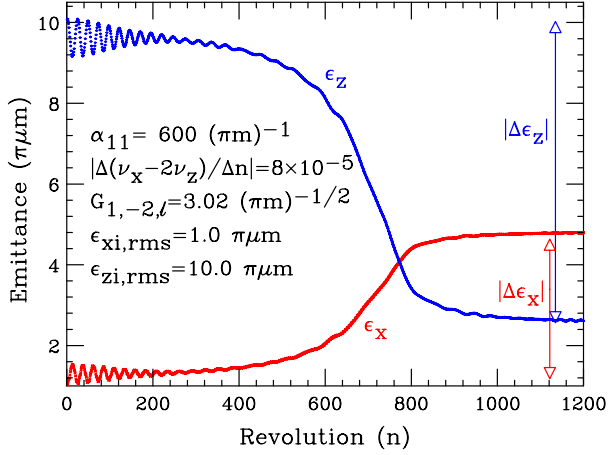


FIG. 4 (color online). The resonance crossing rate is  $-8.0 \times 10^{-5}$  for a third-integer difference resonance of strength  $G_{1,-2,\ell} = 3.02 (\pi \text{mm})^{-1/2}$ ,  $\epsilon_{xi} = 1.0 \pi \mu\text{m}$ , and  $\epsilon_{zi} = 10.0 \pi \mu\text{m}$ . The detuning parameter is fixed at  $\alpha_{11} = 600 (\pi \text{mm})^{-1}$ .

horizontal and vertical phase spaces. If the initial beam distribution in the horizontal and vertical planes is independent and has the same functional form, i.e.,  $\rho_3(J_x, J_z) = f(J_x/\epsilon_x)f(J_z/\epsilon_z)$ , the corresponding beam distribution function  $\rho_{3a}(u, J_2)$  will be symmetric in the  $u$  variable at  $\epsilon_x \approx \frac{1}{2}\epsilon_z$ . Thus, there will be no net emittance exchange because there are an equal number of particles that increase or decrease their actions in crossing the resonance.

In conclusion, multiparticle simulations and Hamiltonian dynamics are employed to study beam properties in crossing a Walkinshaw resonance. We find that the emittance growth obeys a scaling law depending essentially on a dimensionless effective resonance strength parameter:  $G_{1,-2,\ell}\sqrt{\epsilon_{xi}}|\Delta(\nu_x - 2\nu_z)/\Delta n|^{-1/2}$  (see Fig. 3), which is detuning-parameter-independent. The FEG reaches a maximum saturation value at large effective resonance strengths. The maximum FEG depends essentially on  $\epsilon_{xi}/\epsilon_{zi}$ . For  $2\epsilon_{xi} \gg \epsilon_{zi}$ , the maximum FEG is  $2\epsilon_{xi}/\epsilon_{zi}$ , and, for  $2\epsilon_{xi} \ll \epsilon_{zi}$ , the maximum FEG is  $\epsilon_{zi}/(2\epsilon_{xi})$ , as shown in Fig. 5. If the initial emittances of the beam are known, one can predict the emittances after crossing a strong third-integer coupling resonance.

To avoid emittance exchange in passing through a Walkinshaw resonance, we can prepare a beam with an initial horizontal emittance equal to half of the vertical. The minimization of emittance growths and beam loss crossing a Walkinshaw resonance could hopefully lead to an improvement in beam currents in circular accelerators.

Now, we consider a beam with equal initial horizontal and vertical emittance  $\epsilon_0$ . After passing through a strong  $\nu_x - 2\nu_z = \ell$  resonance, the final emittances will be  $\epsilon_x \approx \frac{1}{2}\epsilon_0$  and  $\epsilon_z \approx 2\epsilon_0$ . If the vertical aperture is not an issue, the smaller horizontal emittance can pass through a smaller magnetic or electric septum gap. If this resulting beam is made to pass through the same resonance again at a similarly strong strength, the horizontal emittance and vertical emittance will be exchanged again and restored

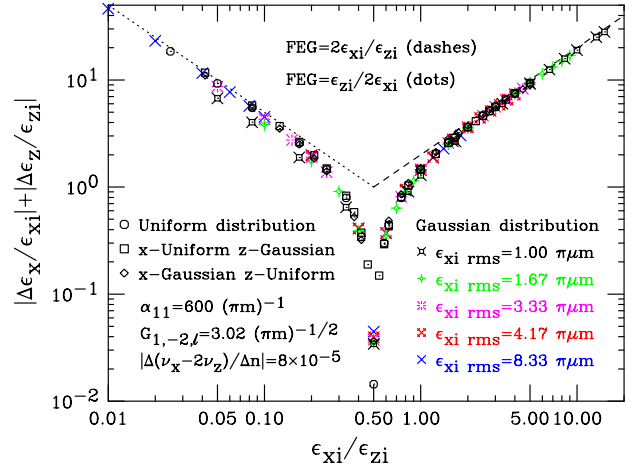


FIG. 5 (color online). The maximum FEG vs  $\epsilon_{xi}/\epsilon_{zi}$ . The dashed and dotted lines correspond to  $\text{FEG}_{\text{max}} \approx 2\epsilon_{xi}/\epsilon_{zi}$  and  $\epsilon_{zi}/2\epsilon_{xi}$ . Note that, near  $\epsilon_{xi} \sim 0.5\epsilon_{zi}$ , there is no emittance exchange. The circle, rectangular, and diamond symbols correspond to uniform distribution in both or one of the transverse phase spaces, and all other data are obtained from bi-Gaussian distribution.

to their original values; i.e., the final beam emittances are  $\epsilon_x \approx \epsilon_z \sim \epsilon_0$ . All these predictions can be tested experimentally in cyclotrons or circular accelerators.

This work is supported in part by grants from the U.S. DOE, under Contracts No. DE-FG02-12ER41800 and No. DE-AC-02-76CH030000, and from the National Science Foundation, Grant No. NSF PHY-1205431. We thank M. Craddock and R. Baartman for many useful comments.

- [1] S. Turner, CERN Report No. 96-02, 1996.
- [2] A.A. Garren, D.L. Judd, L. Smith, and H.A. Willax, *Nucl. Instrum. Methods Phys. Res.* **18-19**, 525 (1962).
- [3] K. Symon, in *Applied Hamiltonian Dynamics*, edited by M. Month and M. Dienes, AIP Conf. Proc. No. 149 (AIP, New York, 1992), p. 370; ANL Report No. LS-132, 1988 (unpublished).
- [4] J. Liu, E. Crosbie, L. Teng, J. Bridges, D. Ciarlette, K. Symon, and W. Trzeciak, *Part. Accel.* **41**, 1 (1993).
- [5] M. Ellison, M. Ball, B. Brabson, J. Budnick, D.D. Caussyn, A.W. Chao, V. Derenchuk, S. Dutt *et al.*, *Phys. Rev. E* **50**, 4051 (1994).
- [6] See, e.g., S. Y. Lee, *Accelerator Physics* (World Scientific, Singapore, 2011), 3rd ed.
- [7] The definition of the FEG is not unique. One may also define it as  $|\Delta\epsilon_x/\epsilon_{xi}|$ , as  $|\Delta\epsilon_z/\epsilon_{zi}|$ , or simply as  $|\Delta\epsilon_x/\epsilon_{xi} + \Delta\epsilon_z/\epsilon_{zi}|$ . Since  $\Delta\epsilon_x$  and  $\Delta\epsilon_z$  are opposite in sign, some of these definitions may not provide the scaling properties shown in Fig. 5.
- [8] S. Y. Lee, *Phys. Rev. Lett.* **97**, 104801 (2006); S. Y. Lee, G. Franchetti, I. Hofmann, F. Wang, and L. Yang, *New J. Phys.* **8**, 291 (2006); S. Y. Lee, K. Y. Ng, X. Pang, Y. Jing, and T. Luo, *Proceedings of HB2012*, Beijing, 2012 (unpublished).